Identification of favourable silica surface sites for single-molecule magnets

Moritz Bernhardt, Lukas Lätsch, Boris Leguennic, Christophe Copéret

Helvetica Chimica Acta
HELVETICA
10.1002/hlca.202300130

Identification of favourable silica surface sites for single-molecule magnets

Moritz Bernhardt,[a] Lukas Lätsch,[a] Boris Le Guennic*,[b] and Christophe Copéret*[a]

[a] Department of Chemistry and Applied Biosciences, ETH Zürich, Vladimir-Prelog Weg 1-5/10, 8093 Zürich, Switzerland
[b] Univ Rennes, CNRS, ISCR (Institut des Sciences Chimiques de Rennes), UMR 6226, 35000 Rennes, France
boris.leguennic@univ-rennes.fr, ccoperet@ethz.ch

Industrial data storage application based on single-molecular magnets (SMMs) necessitates not only strong magnetic remanence at high temperatures but also requires the implementation of the SMM into a solid material to increase their durability and addressability. While the understanding of the relationship between the local structure of the metal and the resulting magnetic behaviour is well understood in molecular systems, it remains challenging to establish a similar understanding for magnetic materials, especially for isolated lanthanide sites on surfaces. For instance, dispersed Dy(III) ions on silica prepared *via* surface organometallic chemistry exhibit slow magnetic relaxation at low temperatures, but the origin of these properties remains unclear. In this work, we modelled ten neutral complexes with coordination numbers (CN) between three and six ([Dy(OSiF$_3$)$_3$(O(SiF$_3$/$_2$)$_{CN-3}$]) representing possible surface sites for dispersed Dy(III) ions and investigated their SMM potential *via ab initio* CASSCF/RASSI-SO calculations. Detailed analysis of the data shows the strong influence of the spatial position of the anionic ligands while the neutral ligands only play a minor role for the magnetic properties. In particular, a T-shape like orientation of the anionic ligands is predicted to exhibit good SMM properties making it a promising targeted coordination environment for molecular and surface-based SMMs.

Keywords: Single-molecule magnetism, Computational chemistry, Lanthanide

Introduction

The interest in single-molecule magnets (SMMs) has steadily increased in recent years, driven by their potential applications in high-density storage media, quantum computing (qbits), and spintronics.[1-4] These molecular entities possess a remarkable feature known as magnetic remanence of purely molecular origin, which arises from their slow magnetic relaxation in the absence of a magnetic field. Lanthanides, especially Dy(III) ions, have been recognized as the most promising candidates for SMMs, due to their high intrinsic magnetic moment in combination with a strong magnetic anisotropy resulting from the ligand-driven crystal field (CF).[5-7] The main challenge in the development of lanthanide-based SMMs lies in tailoring their coordination environment (which is influenced by the special orientation of the ligands,[7] coordination number[8, 9] and potential counter ions[10]) to stabilize a ground state with high spin-orbit coupling (high m_J value). In this context, Rinehart and Long[7] published a landmark paper providing an easy design guideline for the coordination environment needed around every Ln(III) ion to stabilise their highest m_J level as a ground state. This design concept is based on the strong angular dependence of the 4f orbitals, resulting in distinct electron density distribution for every lanthanide, e.g. the m_J=15/2 state of Dy(III) is oblate while it is prolate for Er(III). The stabilisation of these states is achieved by minimising the repulsion between 4f and the ligand electrons, leading to a preferential axial coordination for Dy(III) and equatorial for Er(III) compounds. This design principle has been successfully demonstrated in numerous high-performing SMMs in recent years.[11-18] Synthesizing compounds with a pure axial field (bond angle close to 180 °) which would be beneficial for Dy(III) SMMs has proven to be challenging from an experimental standpoint. Consequently, alternative coordination geometries have garnered attention and extensive investigations. These geometries often involve a combination of strong, nearly axial ligands with short metal-ligand distances, alongside multiple weaker equatorial ligands characterized by longer bond lengths as for example in pentagonal bipyramidal[19-22] or octahedral[19, 23] structures. Although pure axial coordination remains elusive, these alternative geometries offer possibilities to fine-tune the magnetic properties of the compounds and thus, investigating and understanding these non-ideal coordination geometries gives a general understanding of magnetic properties and structure-property relationships.

However, the utilization of SMMs in commercial applications would require converting these molecular entities into supported systems to enhance individual addressability and stability of the magnetic centres.[24, 25]

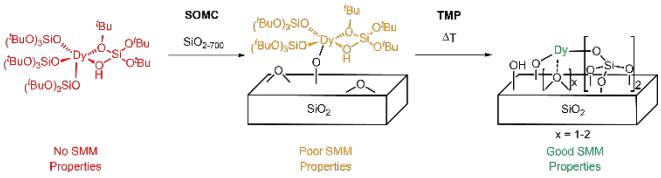

Figure 1. Schematic representation of the SOMC and TMP approaches for ([Dy(OSi(OtBu)$_3$)$_3$(κ$_2$-HOSi(OtBu)$_3$]) on partially dehydroxylated amorphous silica. The colours indicate no (red), poor (orange) and good (green) SMM properties.

Most surface immobilisation methodologies primarily focus on preserving the magnetic properties of the precursor upon surface dispersion[26-37] as even slight alterations of the coordination geometry can diminish or even quench the magnetic performance.[38] An alternative approach was shown by Allouche *et al.* in 2017,[39] where dispersing Dy(III) ions at the surface of silica using a combination of surface organometallic chemistry (SOMC)[40-43] and thermolytic precursors (TMP) was shown to induce SMM properties. SOMC considers the surface functionalities, such as OH groups on oxide supports, as both anchoring sites and potential ligands for the metal sites. During grafting, one anionic ligand of the precursor is typically protonated by a surface OH group and replaced by the resulting surface siloxy group. The remaining organic ligands of the TMP can be removed in a subsequent temperature treatment leading to a completely inorganic material, free of stabilizing organic ligands. Even though this approach is mainly used in the context of catalysis, Allouche and co-worker showed that ([Dy(OSi(OtBu)$_3$)$_3$(κ^2-HOSi(OtBu)$_3$]) not only is a suitable precursor for this methodology (see **Fig.** 1) but also provides a material with SMM properties, albeit displaying a distribution of magnetic relaxation times. Notably, the precursor does not exhibit any slow magnetic relaxation. Experimental investigation of the surface species of the thermolysed material *via* X-ray absorption spectroscopy and solid-state NMR of the Y-analogue revealed a wide distribution of metal sites on the amorphous support with coordination numbers (CN) of metal ions ranging from three up to five surface ligands explaining the observed relaxation time distribution caused by the substantial rearrangements processes of the support initiated by the thermolysis step. So far, the origin of the magnetic properties in the material remains unclear due to the unknown structure of the magnetic surface sites, thus prohibiting the establishment of a structure-property relationship for this material. Similarly, it was shown, that using the same SOMC and TMP approach yields comparable surface chemistry and materials for other rare earth metals like Yb(III) or Eu(III). Namely, these surface dispersed metal ions bound to an antenna ligand display a wide distribution of luminescence properties, paralleling the findings for the magnetic Dy(III) containing material[44] and suggesting a distribution of

surface sites. Furthermore, the corresponding Cr(III) system, which is used as a model system for the Phillips polymerisation catalysts, also shows a distribution of sites as evidenced by the broad polyethlene molecular weight distribution.[45, 46] These additional examples highlight that the analysis of surface species is not only interesting in the field of SMMs but also could open a gateway towards understanding other properties.

Determination of the magnetically active surface sites and understanding their SMM properties pose significant challenges due to the high sensitivity of the magnetic properties towards subtle changes in the ligand environment and the lack of techniques for the determination of the coordination sphere around single metal centres on surfaces. Therefore, theoretical investigations have gained increasing interest in the past decade due to their predictive power and the possibility of elucidating magnetic properties. In the context of this work, mainly four key parameters will be discussed to evaluate the magnetic properties. The energy barrier *U*, describes the thermal energy necessary for total relaxation of the magnetisation of a system, plays a crucial role for the slow magnetic relaxation. *U* is influenced by the relaxation probability between the two ground state Kramers doublets (KDs) and the energy splitting of the KDs, where especially the energy difference between the ground and first excited state ($\Delta E_{1,2}$) should be considered. As SMM properties require a degenerated ground state with a high magnetic anisotropy, not only should the highest m_J level be stabilised as ground state and not mix with other levels but also an Ising type magnetic anisotropy ($g_x \approx g_y \approx 0$, $g_z \approx 20$ for Dy(III)) should be achieved. Calculations not only provide insights into the magnetic behaviour of molecular systems, but can also be extended to enable the exploration of different surface species assembled in silico, offering a way to assess a structure-property relationship for supported compounds[36, 37, 47-52] and therefore present a viable way to evaluate what surface coordination environment enable magnetic properties in materials as prepared by Allouche and co-workers.[39]

Here, we carry out an *ab initio* investigation on a series of neutral Dy(III) models of single atoms dispersed on silica with representative coordination geometries of possible surface sites. We show that the magnetic properties primarily arise from specific relative spatial orientation of the anionic ligands, namely it is best to have two of the three anionic ligands in a *trans* position (bond angle L-Dy-L close to 180 °) as it results in a highly anisotropic ground state with good SMM properties. In contrast, the positions of the neutral ligands only play a minor role for the SMM behaviour of the models,[53] but the increasing number of neutral ligands bound to the metal centre lead to weaker magnetic performances.

Computational details

The model structures of the Y analogues were assembled *in silico* using the Chemcraft software. [54] Geometry optimization calculations of the Y analogue were performed with the Gaussian 09 (revision d1) program suite[55] employing the B3LYP functional[56] in combination with the 6-31g(d) [57] and lanl2dz[58] basis sets for main group elements and Y, respectively. Further the lanl2dz pseudopotential was applied for Y. The initial coordination geometry was chosen to match the respective coordination polyhedron and was optimised freely. In cases where the coordination diverged strongly form the initial orientation upon free optimisation, in subsequent optimisation steps dihedral angles were restricted to ensure the targeted geometry with optimised bond distances (see **Fig.** 2). For all structures frequency analysis were performed to ensure the instigated structure represents a minimum on the potential energy surface.

The calculation of the ^{89}Y chemical shift were performed with the ADF 2014 code[59] using the B3LYP functional[56] including third-generation Grimme's dispersion corrections[60]and Becke–Johnson damping (B3LYP-D3) in combination with a TZP basis set[61] with the all-electron relativistic zeroth-order regular approximation (ZORA)[62-64] in its spin–orbit two-component form. The chemical shift of ^{89}Y derived from the computed shielding is referenced through the previously reported calibration curve of the same method δ_{calc}=-0.727 σ_{calc}+2114.1. [65]

The determination of the magnetic properties involved first replacing Y(III) by Dy(III) without further optimisation of the geometry, followed by the calculation of the electronic structure and magnetic properties using the State-Averaged Complete Active Space Self-Consistent Field approach with Restricted Active Space State Interaction method (SA-CASSCF/RASSI-SO) implemented in the OpenMolcas 19.11 version.[66] The performed multi-configurational approach treated relativistic effects in two steps using the Douglas-Kroll Hamiltonian. In the basis set generation scalar terms are included and are further used in the determination of the CASSCF wave functions and energies.[67] The calculated CASSCF wave functions are mixed within the RASSI-SO method to account for spin-orbit coupling.[68, 69] The active space was selected to encompass the seven 4f orbitals occupied by nine 4f electrons for Dy(III). Within this defined active space, state-averaged CASSCF calculations were performed for all 21 sextets, all 224 quartets and 250 doublets. The resulting excited states were mixed using the RASSI-SO module. The atomic natural (ANO_RCC) basis set was used in the ANO-RCC-VTZP expansion for all atoms.[70, 71] To speed up the calculation and save disc space the Cholesky decomposition of the bielectronic integrals was employed.[72] In the final step, the magnetic properties, the g-tensors of the ground state multiplet and the transition probabilities were computed using the SINGLE_ANISO routine.[73] Visualization of the blocking barrier and the electrostatic potential around the Dy(III) for each model was accomplished using CAMMEL.[74] The CAMMEL code is available under GNU General Public License v3.0 and can be downloaded at https://github.com/rmarchal1/CAMMEL.

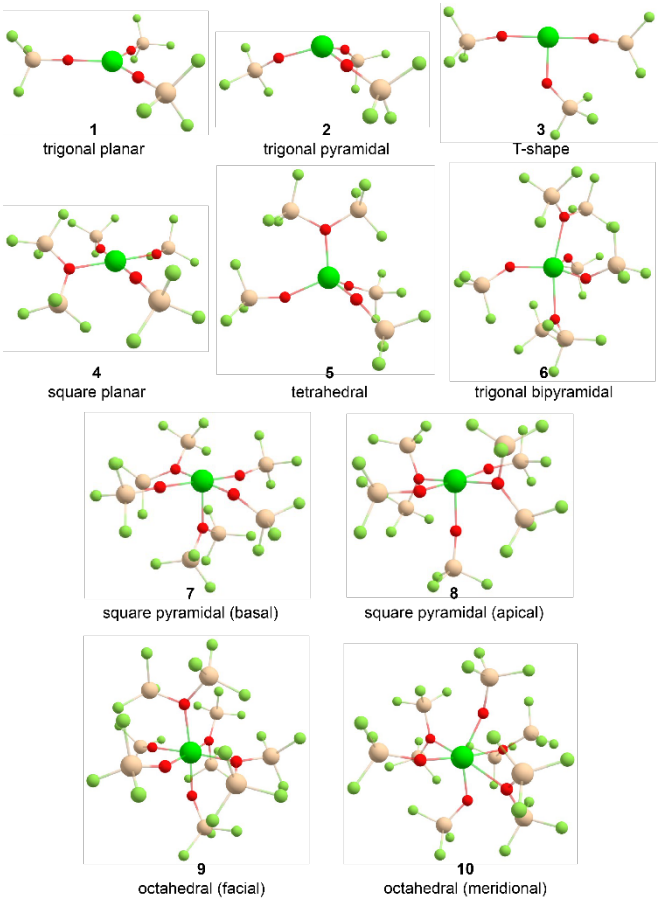

Figure 2. DFT optimised structures for all Y(III) compounds. Colour code: dark green for Y, red for O, brown for Si and light green for F.

10.1002/hlca.202300130

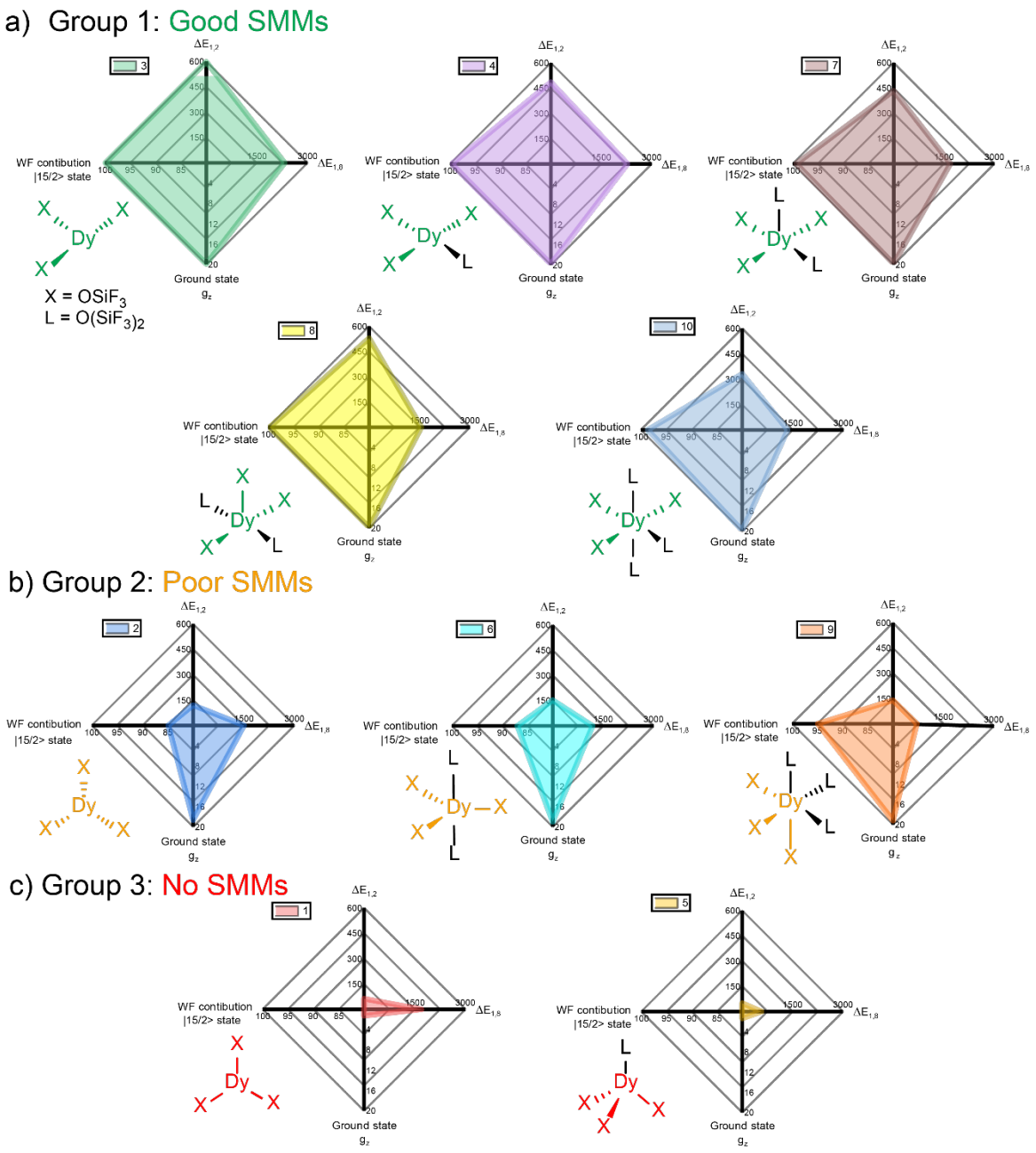

Figure 3. Radar charts for the compounds **1** to **10** including selected features related to their magnetic properties such as $\Delta E_{1,2}$ (top), the energy barrier $\Delta E_{1,8}$ (right), the anisotropy of the g-tensor indicated by the g_z value (bottom) and the wave function contribution of the m_J=15/2 state in the lowest KD indicating the mixing of the ground state (left) for a) group 1, b) group 2 and c) group 3. The anionic ligands (X^-) and the metal centre (Dy) are represented in colour to indicate good (green), poor (orange) and no (red) SMM properties; neutral ligands are indicated in black.

Results and Discussion

For a Dy(III) ion immobilised in a silica surface, one can expect various spatial orientations of anionic ligands and additional coordination of neutral ligands leading to a wide variety of possible surface sites. In this study we focus on ten model compounds with representative coordination environment and varying coordination numbers (CN, see **Fig.** 2). Even though lanthanides can exhibit a larger coordination sphere,[75] higher coordination numbers are increasingly unlikely on surfaces and have thus not been investigated. We modelled the structures representing neutral surface species in different coordination environments as follows: the three anionic $(OSiF_3)^-$ ligands were used to represent surface siloxides counteracting the positive charge of the dysprosium ion and for higher coordination, additional neutral ligands – $O(SiF_3)_2$ – were used to simulate coordination of siloxide bridges; all models can be described with the following general formula: $[Dy(OSiF_3)_3(O(SiF_3)_2)_{CN-3}]$. As seen in **Fig**. 2 the investigated surface models display coordination close to trigonal planar (**1**), trigonal pyramidal (**2**), T-shape (**3**), square planar (**4**), tetrahedral (**5**), trigonal bipyramidal (**6**), square pyramidal with all anionic ligands in basal positions (**7**) or one of the anionic ligands in apical position (**8**) as well as octahedral coordination with the anionic ligands in facial (**9**) and meridional positions (**10**).

The geometries of all structures were optimised for the Y(III) analogue and a frequency analysis was performed to guarantee the extracted structure is a minimum on the potential energy surface. The average of the optimised bond distances (see Table S1) between the metal centre and the anionic ligands per model are between 2.06 and 2.14 Å while the average for the neutral ligands was found to be between 2.14 and 2.22 Å. The latter

distance is strongly elongated in compounds **6** and **10** averaging at 2.52 and 2.69 Å, respectively. Thorough analysis of the Y–O bond distances for the anionic and neutral ligands do not show any trend towards coordination number or coordination geometry.

The ^{89}Y NMR chemical shift parameter of the Y compounds were calculated based on the geometry optimised models and the resulting shielding tensor referenced to experimentally measured compounds to benchmark the calculations and extract the chemical shift in ppm as shown by some of us.[65] All ^{89}Y chemical shifts are in the range of 73 and 198 ppm (see Table S.2) which is in line for the experimentally measured signal for dispersed Y(III) ion on silica *via* the SOMC+TMP approach[44] verifying the importance of the model structures and the presented approach.

Next, the Y(III) ion was first substituted by Dy(III) in the optimised structures and CASSCF/RASSI-SO/SINGLE_ANISO calculations were performed to estimate magnetic anisotropy parameters together with the relaxation mechanism. This method is an established and reliable tool for the prediction of the energies, the wave function and the g-tensor for all low lying Kramer doublets for *4f* complexes.[76] For all ten compounds the eight low lying KDs corresponding to the $^6H_{15/2}$ state were calculated and a qualitative picture of the relaxation pathways constructed. The computed results (see SI) allow the analysis of the compounds in terms of predicted magnetic behaviour which leads to the classification of three categories:

1.) The compounds of the first category (**3**, **4**, **7**, **8** and **10**) with the most promising magnetic properties – slow magnetic relaxation due to a high calculated $\Delta E_{1,2}$ in combination with almost pure m_J=15/2 ground states, exhibiting strong axial anisotropy and low relaxation probabilities between low-lying KDs – possess two anionic ligands arranged with a bond angle close to 180 °. Compound **3** is the simplest of the mentioned examples exhibiting a perfect T-shape orientation of the ligands without additional coordination. As shown in **Fig.** 3 and Table S5 the CF exhibited by the dysprosium ion is strongly axial with pure Ising type anisotropy (g_z=19.9) and a pure m_J=15/2wave function for the GS KD. Even the first and second excited states show strong axial character with pure WF contributions of 13/2 and 11/2, respectively while the fourth KD shows a strong equatorial CF. An additional positive factor are the high energy differences between the first four Kramers doublets in combination with a negligible relaxation probability between the lowest three states. Therefore, the most likely relaxation pathway is going through the fourth state resulting in a high energy barrier *U* and consequently leads to slow magnetic relaxation (see **Fig.** S5). Due to geometric restrictions for all other models in this group, the anionic ligands and the Dy(III) ion form a T-shape coordination which dominates the coordination environment with only little influence of the position of the neutral ligands. In the case of the square planar coordination (**4**), the addition of a neutral ligand results in similar ground state values in terms of anisotropy and WF composition as for compound **3** (see **Fig.** 1.3, Table S6). Differences occur in the excited states where a higher mixing of the wave function in combination with a more equatorial crystal field and a slightly reduced $\Delta E_{1,2}$ can be observed. This leads to a higher probability of relaxation through the first excited state strongly reducing *U* compared to **3** (see **Fig.** S7). Further increasing the number of neutral ligand leads to a decrease of $\Delta E_{1,2}$ as seen for **7** and **10** were the latter one shows the lowest overall energy splitting for the eight low-lying KDs corresponding to the $^6H_{15/2}$ state with 1345 cm^{-1}. Interestingly, even though the energy splitting and $\Delta E_{1,2}$ in the meridional octahedral structures are smaller than for **4**, the first excited state is characterised by a strong axial coordination, only minor mixing of the wave function and low transition probabilities (see **Fig.** 3, Table S12 and **Fig.** S19 and S20). This should lead to a relaxation *via* the third excited state in **10** and consequently lead to a higher *U* compared to **4**. Not only the number of ligands and their orientation in the complex but also the relative position to each other has an influence on the overall magnetic performance as seen by comparing the square pyramidal models **7** and **8**. In **7** all three anionic ligands are located in basal positions while for **8** one anionic ligand occupies the apical position with the other two in basal positions trans to each other. In both cases the remaining two coordination sites are occupied by neutral ligands. The characteristic structural T-shape form is present in both cases while for **8** the apical ligand is slightly bend leading to L_{basal}–Dy–L_{apical} angle of 97.7 ° and 87.3 ° reducing the coordination strength in the equatorial position and consequently, a higher energy splitting between the KDs can be observed. Additionally, **8** shows relatively pure states up to the second excited state with strong axiality and low probability of relaxation up to the fourth KD.

2.) The second group comprises compounds **2**, **6** and **9** with predicted weak magnetic properties due to a trigonal coordination of the three anionic ligands. Such configuration leads to the stabilisation of m_J=15/2 as main component of the ground state with a fairly axial crystal field ($g_z \sim 19$); the resulting strong mixing of the states in the ground and especially the excited energy levels for all three models (see **Fig.** 3, Tables S3, S7 and S10) lead however to an overall small energy barrier (*U*) between lowest KDs and to non-negligible relaxation contribution for QTM and Raman/Orbach processes especially in the ground and first excited states (see **Fig.** S3, S11 and S17). Therefore, only weak SMM properties are to be expected for these compounds due to fast relaxation *via* low-lying m_J level. In detail, the divergence from the trigonal planar coordination (like in **1**) to a more pyramidal orientation in compound **2** leads to the stabilisation of m_J=15/2 as ground state and a higher $\Delta E_{1,2}$ due to the strong influence of two anionic ligands (see **Fig.** S4) representing a better geometry for SMM properties. In the case of the facial octahedron, the coordination of **9** has strong similarities to compound **2** with smaller bond angles between the anionic ligands and three additional neutral ligands The reduced bond angles influence the electronic structure towards higher purity of states and slightly higher $\Delta E_{1,2}$ compared to **2**. As for **6**, the influence of the two neutral ligands in the apical position is negligible (see **Fig.** S12) while the almost trigonal planar orientation of the anionic ligands shows bond angles between 113 and 124 ° leading to a more axial field than for compound **1**. This deviation from the perfect trigonal planar orientation of the anionic ligands results in the found change of ground state compared to **1**.

3.) The third group consists of all compounds in a strong equatorial crystal field which are expected to display no magnetic properties with the stabilisation of the lowest m_J state (1/2) of Dy(III). Compounds **1** and **5** are both assigned to this category based on the stabilised ground and excited states wave function contributions. Furthermore, the low $\Delta E_{1,2}$ and non-axial nature of the lower states expressed by the transverse anisotropy of the g-tensor (see **Fig.** 3, Tables S3 and S7) indicate a lack of SMM properties for these structures even at low temperatures. **1** resembles a trigonal planar coordination environment which according to the Rinehart and Long model should be a suitable coordination for a prolate ion like Er(III) while for oblate ions as such Dy(III) poor magnetic behaviour are predicted and corroborated by the calculations. The tetrahedral coordination of **5** is dominated by the influence of the anionic ligands (as seen in the electrostatic potential, see **Fig.** 10) also leading to a strong equatorial CF and hence no SMM behaviour.

Conclusions

In the search for understanding what makes a magnetically active surface deposited Dy(III) ions on silica, we have performed a computational study on ten representative model structures having various coordination geometries using a combination of DFT optimisation and ab initio CASSCF/RASSI-SO/SINGLE_ANISO calculations for the determination of magnetic properties, anisotropy and energy barrier height of magnetisation reversal. The model structures were characterised based on their calculated magnetic properties and enable to classify them into three main groups:

1) The striking feature of the first group is the almost linear ω between two anionic ligands and the metal centre resulting in a T-shape structure for all models. This spatial orientation of the ligands leads to a strong axial crystal field in the ground and partly also in the first excited states accompanied with low relaxation probabilities. Even though, increasing number of ligands slightly diminish the magnetic performance, the magnetic active species generated by the SOMC and TMP approach most likely has a similar coordination sphere as the models present in this group.

2) The trigonal orientation of the anionic ligands in the second group results in the stabilisation of the highest m_J ground state necessary for SMM properties. This significant change results mainly from the divergence from a planar to a more pyramidal coordination of the anionic ligands paired with short distances to one or two of the negatively charged ligands. However, the low $\Delta E_{1,2}$ in combination with strong mixing and non-negligible relaxation probabilities in the lowest KDs most likely leads to a weak magnetic behaviour resulting in limiting these structures to either low temperatures or field induced SMMs.

3) The third group is characterised by the equatorial crystal field experienced by the Dy(III) resulting in the stabilisation of the lowest m_J level and consequently poor to no SMM properties as expected based on the design guideline from Rinehart and Long.

We want to emphasise that the presented approach only contains model compounds which were chosen to be close to the respective polyhedron to model different surface coordination. On the surface and especially after the temperature treatment (as performed in [39]) a distribution of surface sites is present in the material which cannot be fully represented by only these ten model compounds. Notably, investigations of the coordination environment around a Cr(III) ion dispersed on silica, that expected active sites in the Phillips olefin polymerisation catalysts, had also revealed that T-shape structures are also privilege structures that are expected to be highly reactive in olefin polymerization due to the presence of strain,[77, 78] paralleling the expected beneficial effect with similar geometries for the magnetic properties of Dy(III) species dispersed on silica.[36] The similarities between these systems further ascertain that T-shape geometries are likely present on silica surface and provides unique ligand field and functions. Thus, the presented approach not only helped to identify possible magnetic surface structures but also revealed clear structure-property relations for the surface sites. Furthermore, a so far overlooked geometry of SMMs, the T-shape structure, was identified and further investigations towards isolating this coordination, also on the molecular level, might proof an effective way toward high performing SMMs.

Supporting Information

Supporting information for this article contains calculated data for the bond length, NMR chemical shifts and magnetic properties for compounds **1**-**10**.

Acknowledgemments

M.B would like to thank the ETH Zürich Grant program (ETH-44 18-1). L.L. thanks the Scholarship Fund of the Swiss Chemical Industry (SSCI) for funding. B.L.G thanks the European Research Council (ERC-CoG 725184 MULTIPROSMM) and the Agence Nationale de la Recherche (SMMCPL ANR-19-CE29-0012-02).

Author Contribution Statement

M.B. and C.C. conceptualised and designed the project. L.L performed the geometry optimizations and the calculations of the NMR chemical shifts. M.B. and B.L.G. completed the ab initio calculations and processed the results. All authors were involved in writing of the manuscript and approved its final version.

References

[1.] S. T. Liddle, J. van Slageren. 'Improving f-element single molecule magnets.' Chemical Society Reviews 2015, 44, 6655-6669.

[2.] A. Gaita-Ariño, H. Prima-García, S. Cardona-Serra, L. Escalera-Moreno, L. E. Rosaleny, J. J. Baldoví. 'Coherence and organisation in lanthanoid complexes: from single ion magnets to spin qubits.' Inorg. Chem. Front. 2016, 3, 568-577.

[3.] A. Gaita-Ariño, F. Luis, S. Hill, E. Coronado. 'Molecular spins for quantum computation.' Nature Chem. 2019, 11, 301-309.

[4.] L. Bogani, W. Wernsdorfer. 'Molecular spintronics using single-molecule magnets.' Nat Mater 2008, 7, 179-86.

[5.] Y. S. Meng, S. D. Jiang, B. W. Wang, S. Gao. 'Understanding the Magnetic Anisotropy toward Single-Ion Magnets.' Acc. Chem. Res. 2016, 49, 2381-2389.

[6.] D. N. Woodruff, R. E. Winpenny, R. A. Layfield. 'Lanthanide single-molecule magnets.' Chem. Rev. 2013, 113, 5110-48.

[7.] J. D. Rinehart, J. R. Long. 'Exploiting single-ion anisotropy in the design of f-element single-molecule magnets.' Chem. Sci. 2011, 2, 2078-2085.

[8.] A. B. Canaj, M. K. Singh, E. Regincós Marti, M. Damjanović, C. Wilson, O. Céspedes, W. Wernsdorfer, G. Rajaraman, M. Murrie. 'Boosting axiality in stable high-coordinate Dy(iii) single-molecule magnets.' Chem. Commun.2019, 55, 5950-5953.

[9.] S. K. Singh, T. Gupta, M. Shanmugam, G. Rajaraman. 'Unprecedented magnetic relaxation via the fourth excited state in low-coordinate lanthanide single-ion magnets: a theoretical perspective.' Chem. Commun. 2014, 50, 15513-15516.

[10.] I. F. Díaz-Ortega, J. M. Herrera, S. Dey, H. Nojiri, G. Rajaraman, E. Colacio. 'The effect of the electronic structure and flexibility of the counteranions on magnetization relaxation in [Dy(L)2(H2O)5]3+ (L = phosphine oxide derivative) pentagonal bipyramidal SIMs.' Inorg. Chem. Front. 2020, 7, 689-699.

[11.] S. D. Jiang, S. S. Liu, L. N. Zhou, B. W. Wang, Z. M. Wang, S. Gao. 'Series of lanthanide organometallic single-ion magnets.' Inorg. Chem. 2012, 51, 3079-87.

[12.] K. R. Meihaus, J. R. Long. 'Magnetic Blocking at 10 K and a Dipolar-Mediated Avalanche in Salts of the Bis(η8-cyclooctatetraenide) Complex [Er(COT)2]−.' J. Am. Chem.Soc.2013, 135, 17952-17957.

[13.] C. A. P. Goodwin, F. Ortu, D. Reta, N. F. Chilton, D. P. Mills. 'Molecular magnetic hysteresis at 60 kelvin in dysprosocenium.' Nature 2017, 548, 439-442.

[14.] F. S. Guo, B. M. Day, Y. C. Chen, M. L. Tong, A. Mansikkamaki, R. A. Layfield. 'Magnetic hysteresis up to 80 kelvin in a dysprosium metallocene single-molecule magnet.' Science 2018, 362, 1400-1403.

[15.] F. S. Guo, B. M. Day, Y. C. Chen, M. L. Tong, A. Mansikkamaki, R. A. Layfield. 'A Dysprosium Metallocene Single-Molecule Magnet Functioning at the Axial Limit.' Angew. Chem. Int. Ed. 2017, 56, 11445-11449.

[16.] S. D. Jiang, B. W. Wang, H. L. Sun, Z. M. Wang, S. Gao. 'An organometallic single-ion magnet.' J. Am. Chem. Soc. 2011, 133, 4730-3.

[17.] C. A. Gould, K. R. McClain, D. Reta, J. G. C. Kragskow, D. A. Marchiori, E. Lachman, E. S. Choi, J. G. Analytis, R. D. Britt, N. F. Chilton, B. G. Harvey, J. R. Long. 'Ultrahard magnetism from mixed-valence dilanthanide complexes with metal-metal bonding.' Science 2022, 375, 198-202.

[18.] C. A. Gould, K. R. McClain, J. M. Yu, T. J. Groshens, F. Furche, B. G. Harvey, J. R. Long. 'Synthesis and Magnetism of Neutral, Linear Metallocene Complexes of Terbium(II) and Dysprosium(II).' J. Am. Chem. Soc. 2019, 141, 12967-12973.

[19.] J.-L. Liu, Y.-C. Chen, Y.-Z. Zheng, W.-Q. Lin, L. Ungur, W. Wernsdorfer, L. F. Chibotaru, M.-L. Tong. 'Switching the anisotropy barrier of a single-ion magnet by symmetry change from quasi-D5h to quasi-Oh.' Chem. Sci. 2013, 4, 3310-3316.

[20.] Y. C. Chen, J. L. Liu, L. Ungur, J. Liu, Q. W. Li, L. F. Wang, Z. P. Ni, L. F. Chibotaru, X. M. Chen, M. L. Tong. 'Symmetry-Supported Magnetic Blocking at 20 K in Pentagonal Bipyramidal Dy(III) Single-Ion Magnets.' J. Am. Chem. Soc. 2016, 138, 2829-37.

[21.] J.-P. Sutter, V. Béreau, V. Jubault, K. Bretosh, C. Pichon, C. Duhayon. 'Magnetic anisotropy of transition metal and lanthanide ions in pentagonal bipyramidal geometry.' Chem.Soc. Rev. 2022, 51, 3280-3313.

[22.] S. K. Gupta, S. Dey, T. Rajeshkumar, G. Rajaraman, R. Murugavel. 'Deciphering the Role of Anions and Secondary Coordination Sphere in Tuning Anisotropy in Dy(III) Air-Stable D5h SIMs.' Chem. Eur. J. 2022, 28, e202103585.

[23.] C. Das, A. Upadhyay, M. Shanmugam. 'Influence of Radicals on Magnetization Relaxation Dynamics of Pseudo-Octahedral Lanthanide Iminopyridyl Complexes.' Inorganic Chemistry 2018, 57, 9002-9011.

[24.] K. L. M. Harriman, D. Errulat, M. Murugesu. 'Magnetic Axiality: Design Principles from Molecules to Materials.' Trends Chem. 2019, 1, 425-439.
[25.] J. Dreiser. 'Molecular lanthanide single-ion magnets: from bulk to submonolayers.' J. Phys. Condens. Matter. 2015, 27, 183203.
[26.] J. Gomez-Segura, J. Veciana, D. Ruiz-Molina. 'Advances on the nanostructuration of magnetic molecules on surfaces: the case of single-molecule magnets (SMM).' Chem. Commun. 2007, 3699-707.
[27.] M. Mannini, F. Pineider, P. Sainctavit, C. Danieli, E. Otero, C. Sciancalepore, A. M. Talarico, M. A. Arrio, A. Cornia, D. Gatteschi, R. Sessoli. 'Magnetic memory of a single-molecule quantum magnet wired to a gold surface.' Nat. Mater. 2009, 8, 194-7.
[28.] C. Gimenez-Lopez M. del, F. Moro, A. La Torre, C. J. Gomez-Garcia, P. D. Brown, J. van Slageren, A. N. Khlobystov. 'Encapsulation of single-molecule magnets in carbon nanotubes.' Nat. Commun. 2011, 2, 407.
[29.] M. Perfetti, F. Pineider, L. Poggini, E. Otero, M. Mannini, L. Sorace, C. Sangregorio, A. Cornia, R. Sessoli. 'Grafting single molecule magnets on gold nanoparticles.' Small 2014, 10, 323-9.
[30.] F. Donati, S. Rusponi, S. Stepanow, C. Wackerlin, A. Singha, L. Persichetti, R. Baltic, K. Diller, F. Patthey, E. Fernandes, J. Dreiser, Z. Sljivancanin, K. Kummer, C. Nistor, P. Gambardella, H. Brune. 'Magnetic remanence in single atoms.' Science 2016, 352, 318-21.
[31.] R. Baltic, M. Pivetta, F. Donati, C. Wäckerlin, A. Singha, J. Dreiser, S. Rusponi, H. Brune. 'Superlattice of Single Atom Magnets on Graphene.' Nano Lett. 2016, 16, 7610-7615.
[32.] C. Wackerlin, F. Donati, A. Singha, R. Baltic, S. Rusponi, K. Diller, F. Patthey, M. Pivetta, Y. Lan, S. Klyatskaya, M. Ruben, H. Brune, J. Dreiser. 'Giant Hysteresis of Single-Molecule Magnets Adsorbed on a Nonmagnetic Insulator.' Adv. Mater. 2016, 28, 5195-9.
[33.] V. E. Campbell, M. Tonelli, I. Cimatti, J. B. Moussy, L. Tortech, Y. J. Dappe, E. Riviere, R. Guillot, S. Delprat, R. Mattana, P. Seneor, P. Ohresser, F. Choueikani, E. Otero, F. Koprowiak, V. G. Chilkuri, N. Suaud, N. Guihery, A. Galtayries, F. Miserque, M. A. Arrio, P. Sainctavit, T. Mallah. 'Engineering the magnetic coupling and anisotropy at the molecule-magnetic surface interface in molecular spintronic devices.' Nat. Commun. 2016, 7, 13646.
[34.] F. D. Natterer, K. Yang, W. Paul, P. Willke, T. Choi, T. Greber, A. J. Heinrich, C. P. Lutz. 'Reading and writing single-atom magnets.' Nature 2017, 543, 226-228.
[35.] L. Spree, F. P. Liu, V. Neu, M. Rosenkranz, G. Velkos, Y. F. Wang, S. Schiemenz, J. Dreiser, P. Gargiani, M. Valvidares, C. H. Chen, B. Buchner, S. M. Avdoshenko, A. A. Popov, H. Chen. 'Robust Single Molecule Magnet Monolayers on Graphene and Graphite with Magnetic Hysteresis up to 28 K.' Adv. Funct. Mater. 2021, 31, 2105516.
[36.] M. D. Korzynski, Z. J. Berkson, B. Le Guennic, O. Cador, C. Coperet. 'Leveraging Surface Siloxide Electronics to Enhance the Relaxation Properties of a Single-Molecule Magnet.' J. Am. Chem. Soc. 2021, 143, 5438-5444.
[37.] M. Bernhardt, M. D. Korzynski, Z. J. Berkson, F. Pointillart, B. Le Guennic, O. Cador, C. Coperet. 'Tailored Lewis Acid Sites for High-Temperature Supported Single-Molecule Magnetism.' J. Am. Chem. Soc. 2023, 145, 12446-12451.
[38.] R. J. Holmberg, M. Murugesu. 'Adhering magnetic molecules to surfaces.' Journal of Materials Chemistry C 2015, 3, 11986-11998.
[39.] F. Allouche, G. Lapadula, G. Siddiqi, W. W. Lukens, O. Maury, B. Le Guennic, F. Pointillart, J. Dreiser, V. Mougel, O. Cador, C. Coperet. 'Magnetic Memory from Site Isolated Dy(III) on Silica Materials.' ACS Cent. Sci. 2017, 3, 244-249.
[40.] C. Coperet. 'Single-Sites and Nanoparticles at Tailored Interfaces Prepared via Surface Organometallic Chemistry from Thermolytic Molecular Precursors.' Acc. Chem. Res. 2019, 52, 1697-1708.
[41.] C. Copéret, F. Allouche, K. W. Chan, M. P. Conley, M. F. Delley, A. Fedorov, I. B. Moroz, V. Mougel, M. Pucino, K. Searles, K. Yamamoto, P. A. Zhizhko. 'Bridging the Gap between Industrial and Well-Defined Supported Catalysts.' Angew. Chem., Int. Ed. 2018, 57, 6398-6440.
[42.] C. Copéret, M. Chabanas, R. Petroff Saint-Arroman, J.-M. Basset. 'Homogeneous and Heterogeneous Catalysis: Bridging the Gap through Surface Organometallic Chemistry.' Angew. Chem., Int. Ed. 2003, 42, 156-181.
[43.] C. Coperet, A. Comas-Vives, M. P. Conley, D. P. Estes, A. Fedorov, V. Mougel, H. Nagae, F. Nunez-Zarur, P. A. Zhizhko. 'Surface Organometallic and Coordination Chemistry toward Single-Site Heterogeneous Catalysts: Strategies, Methods, Structures, and Activities.' Chem. Rev. 2016, 116, 323-421.
[44.] M. F. Delley, G. Lapadula, F. Núñez-Zarur, A. Comas-Vives, V. Kalendra, G. Jeschke, D. Baabe, M. D. Walter, A. J. Rossini, A. Lesage, L. Emsley, O. Maury, C. Copéret. 'Local Structures and Heterogeneity of Silica-Supported M(III) Sites Evidenced by EPR, IR, NMR, and Luminescence Spectroscopies.' J. Am. Chem. Soc. 2017, 139, 8855-8867.
[45.] M. F. Delley, F. Núñez-Zarur, M. P. Conley, A. Comas-Vives, G. Siddiqi, S. Norsic, V. Monteil, O. V. Safonova, C. Copéret. 'Proton transfers are key elementary steps in ethylene polymerization on isolated chromium(III) silicates.' Proc. Natl. Acad. Sci. 2014, 111, 11624-11629.
[46.] M. F. Delley, M.-C. Silaghi, F. Nuñez-Zarur, K. V. Kovtunov, O. G. Salnikov, D. P. Estes, I. V. Koptyug, A. Comas-Vives, C. Copéret. 'X–H Bond Activation on Cr(III),O Sites (X = R, H): Key Steps in Dehydrogenation and Hydrogenation Processes.' Organomet. 2017, 36, 234-244.
[47.] F. Totti, G. Rajaraman, M. Iannuzzi, R. Sessoli. 'Computational Studies on SAMs of {Mn6} SMMs on Au(111): Do Properties Change upon Grafting?', J. Phys. Chem. C 2013, 117, 7186-7190.
[48.] A. Lunghi, M. Iannuzzi, R. Sessoli, F. Totti. 'Single molecule magnets grafted on gold: magnetic properties from ab initio molecular dynamics.' J. Mater. Chem. C 2015, 3, 7294-7304.
[49.] I. Cimatti, X. Yi, R. Sessoli, M. Puget, B. L. Guennic, J. Jung, T. Guizouarn, A. Magnani, K. Bernot, M. Mannini. 'Chemical tailoring of Single Molecule Magnet behavior in films of Dy(III) dimers.' Appl. Surf. Sci. 2018, 432, 7-14.
[50.] X. Yi, F. Pointillart, B. Le Guennic, J. Jung, C. Daiguebonne, G. Calvez, O. Guillou, K. Bernot. 'Rational engineering of dimeric Dy-based Single-Molecule Magnets for surface grafting.' Polyhedron 2019, 164, 41-47.
[51.] R. Nabi, R. K. Tiwari, G. Rajaraman. 'In silico strategy to boost stability, axiality, and barrier heights in dysprocenium SIMs via SWCNT encapsulation.' Chem. Commun. 2021, 57, 11350-11353.
[52.] T. Sharma, M. K. Singh, R. Gupta, M. Khatua, G. Rajaraman. 'In silico design to enhance the barrier height for magnetization reversal in Dy(iii) sandwich complexes by stitching them under the umbrella of corannulene.' Chem. Sci. 2021, 12, 11506-11514.
[53.] D. Aravena, E. Ruiz. 'Shedding Light on the Single-Molecule Magnet Behavior of Mononuclear DyIII Complexes.' Inorg. Chem. 2013, 52, 13770-13778.
[54.] 'Chemcraft - graphical software for visualization of quantum chemistry computations. Version 1.8, build 648. https://www.chemcraftprog.com.'
[55.] R. D. Gaussian 09, M. J. Frisch, G. W. Trucks, H. B. Schlegel, G. E. Scuseria, M. A. Robb, J. R. Cheeseman, G. Scalmani, V. Barone, G. A. Petersson, H. Nakatsuji, X. Li, M. Caricato, A. Marenich, J. Bloino, B. G. Janesko, R. Gomperts, B. Mennucci, H. P. Hratchian, J. V. Ortiz, A. F. Izmaylov, J. L. Sonnenberg, D. Williams-Young, F. Ding, F. Lipparini, F. Egidi, J. Goings, B. Peng, A. Petrone, T. Henderson, D. Ranasinghe, V. G. Zakrzewski, J. Gao, N. Rega, G. Zheng, W. Liang, M. Hada, M. Ehara, K. Toyota, R. Fukuda, J. Hasegawa, M. Ishida, T. Nakajima, Y. Honda, O. Kitao, H. Nakai, T. Vreven, K. Throssell, J. A. Montgomery, Jr., J. E. Peralta, F. Ogliaro, M. Bearpark, J. J. Heyd, E. Brothers, K. N. Kudin, V. N. Staroverov, T. Keith, R. Kobayashi, J. Normand, K. Raghavachari, A. Rendell, J. C. Burant, S. S. Iyengar, J. Tomasi, M. Cossi, J. M. Millam, M. Klene, C. Adamo, R. Cammi, J. W. Ochterski, R. L. Martin, K. Morokuma, O. Farkas, J. B. Foresman, and D. J. Fox, Gaussian, Inc., Wallingford CT, 2016.
[56.] A. D. Becke. 'Density ‐ functional thermochemistry. III. The role of exact exchange.' J. Chem. Phys. 1993, 98, 5648-5652.

[57.] W. J. Hehre, R. Ditchfield, J. A. Pople. 'Self—Consistent Molecular Orbital Methods. XII. Further Extensions of Gaussian—Type Basis Sets for Use in Molecular Orbital Studies of Organic Molecules.' J. Chem. Phys. 2003, 56, 2257-2261.
[58.] L. E. Roy, P. J. Hay, R. L. Martin. 'Revised Basis Sets for the LANL Effective Core Potentials.' J Chem Theory Comput 2008, 4, 1029-1031.
[59.] G. te Velde, F. M. Bickelhaupt, E. J. Baerends, C. Fonseca Guerra, S. J. A. van Gisbergen, J. G. Snijders, T. Ziegler. 'Chemistry with ADF.' J Comput. Chem. 2001, 22, 931-967.
[60.] S. Grimme, J. Antony, S. Ehrlich, H. Krieg. 'A consistent and accurate ab initio parametrization of density functional dispersion correction (DFT-D) for the 94 elements H-Pu.' J. Chem. Phys. 2010, 132.
[61.] E. Van Lenthe, E. J. Baerends. 'Optimized Slater-type basis sets for the elements 1–118.' J. Comput. Chem. 2003, 24, 1142-1156.
[62.] E. v. Lenthe, E. J. Baerends, J. G. Snijders. 'Relativistic regular two - component Hamiltonians.' J. Chem. Phys. 1993, 99, 4597-4610.
[63.] E. van Lenthe, A. Ehlers, E.-J. Baerends. 'Geometry optimizations in the zero order regular approximation for relativistic effects.' J. Chem. Phys. 1999, 110, 8943-8953.
[64.] E. van Lenthe, E. J. Baerends, J. G. Snijders. 'Relativistic total energy using regular approximations.' J. Chem. Phys. 1994, 101, 9783-9792.
[65.] L. Lätsch, E. Lam, C. Copéret. 'Electronegativity and location of anionic ligands drive yttrium NMR for molecular, surface and solid-state structures.' Chem. Sci. 2020, 11, 6724-6735.
[66.] I. Fdez Galvan, M. Vacher, A. Alavi, C. Angeli, F. Aquilante, J. Autschbach, J. J. Bao, S. I. Bokarev, N. A. Bogdanov, R. K. Carlson, L. F. Chibotaru, J. Creutzberg, N. Dattani, M. G. Delcey, S. S. Dong, A. Dreuw, L. Freitag, L. M. Frutos, L. Gagliardi, F. Gendron, A. Giussani, L. Gonzalez, G. Grell, M. Guo, C. E. Hoyer, M. Johansson, S. Keller, S. Knecht, G. Kovacevic, E. Kallman, G. Li Manni, M. Lundberg, Y. Ma, S. Mai, J. P. Malhado, P. A. Malmqvist, P. Marquetand, S. A. Mewes, J. Norell, M. Olivucci, M. Oppel, Q. M. Phung, K. Pierloot, F. Plasser, M. Reiher, A. M. Sand, I. Schapiro, P. Sharma, C. J. Stein, L. K. Sorensen, D. G. Truhlar, M. Ugandi, L. Ungur, A. Valentini, S. Vancoillie, V. Veryazov, O. Weser, T. A. Wesolowski, P. O. Widmark, S. Wouters, A. Zech, J. P. Zobel, R. Lindh. 'OpenMolcas: From Source Code to Insight.' J. Chem. Theory. Comput. 2019, 15, 5925-5964.
[67.] B. O. Roos, P. R. Taylor, P. E. M. Siegbahn. 'A Complete Active Space Scf Method (Casscf) Using a Density-Matrix Formulated Super-Ci Approach.' Chem. Phys. 1980, 48, 157-173.
[68.] P. A. Malmqvist, B. O. Roos. 'The Casscf State Interaction Method.' Chem. Phys. Lett. 1989, 155, 189-194.
[69.] P. A. Malmqvist, B. O. Roos, B. Schimmelpfennig. 'The restricted active space (RAS) state interaction approach with spin-orbit coupling.' Chem. Phys. Lett. 2002, 357, 230-240.
[70.] B. O. Roos, R. Lindh, P. A. Malmqvist, V. Veryazov, P. O. Widmark. 'Main group atoms and dimers studied with a new relativistic ANO basis set.' J. Phys. Chem. A 2004, 108, 2851-2858.
[71.] B. O. Roos, R. Lindh, P. A. Malmqvist, V. Veryazov, P. O. Widmark, A. C. Borin. 'New relativistic atomic natural orbital basis sets for lanthanide atoms with applications to the Ce diatom and LuF3.' J. Phys. Chem. A 2008, 112, 11431-5.
[72.] F. Aquilante, P. A. Malmqvist, T. B. Pedersen, A. Ghosh, B. O. Roos. 'Cholesky Decomposition-Based Multiconfiguration Second-Order Perturbation Theory (CD-CASPT2): Application to the Spin-State Energetics of Co(III)(diiminato)(NPh).' J. Chem. Theory. Comput. 2008, 4, 694-702.
[73.] L. F. Chibotaru, L. Ungur. 'Ab initio calculation of anisotropic magnetic properties of complexes. I. Unique definition of pseudospin Hamiltonians and their derivation.' J. Chem. Phys. 2012, 137, 064112.
[74.] G. Huang, G. Fernandez-Garcia, I. Badiane, M. Camarra, S. Freslon, O. Guillou, C. Daiguebonne, F. Totti, O. Cador, T. Guizouarn, B. Le Guennic, K. Bernot. 'Magnetic Slow Relaxation in a Metal–Organic Framework Made of Chains of Ferromagnetically Coupled Single-Molecule Magnets.' Chem. Eur. J. 2018, 24, 6983-6991.
[75.] W. J. Evans. 'The importance of questioning scientific assumptions: some lessons from f element chemistry.' Inorg Chem 2007, 46, 3435-49.
[76.] A. Swain, A. Sarkar, G. Rajaraman. 'Role of Ab Initio Calculations in the Design and Development of Organometallic Lanthanide-Based Single-Molecule Magnets.' Chem. Asian. J. 2019, 14, 4056-4073.
[77.] L. Floryan, A. P. Borosy, F. Núñez-Zarur, A. Comas-Vives, C. Copéret. 'Strain effect and dual initiation pathway in CrIII/SiO2 polymerization catalysts from amorphous periodic models.' J. Catal. 2017, 346, 50-56.
[78.] F. Núñez-Zarur, A. Comas-Vives. 'Understanding the Olefin Polymerization Initiation Mechanism by Cr(III)/SiO2 Using the Activation Strain Model.' J. Phys. Chem. C 2022, 126, 296-308.

10.1002/hlca.202300130

HELVETICA

Entry for the Table of Contents